ANATOMIA HISTOLOGIA EMBRYOLOGIA
JOURNAL OF VETERINARY MEDICINE
Anatomia Histologia Embryologia

ORIGINAL ARTICLE

Anatomical, Histological and Immunohistochemical Study of the Reproductive System Accessory Glands in Male Viscacha (*Lagostomus maximus maximus*)

E. M. Chaves*,†, C. Aguilera-Merlo, V. Filippa†, F. Mohamed, S. Dominguez and L. Scardapane

Address of authors: Cátedra de Histología, Facultad de Química, Bioquímica y Farmacia, Universidad Nacional de San Luis. Av. Ejército de los Andes 950 - 2° Piso. 5700, San Luis, Argentina

***Correspondence:**
Tel.: +54 2652 424027/266; fax: +54 2652 422644/426756; e-mail: emchaves@unsl.edu.ar

With 6 figures and 1 table

Received December 2009; accepted for publication August 2010

doi: 10.1111/j.1439-0264.2010.01032.x

†Fellow of the Research Career, Consejo Nacional de Investigaciones Científicas y Técnicas (CONICET), Argentina.

Summary

The anatomy, histology and androgen receptor immunohistochemistry of the prostate (P), seminal vesicles (SV), bulbourethral and coagulant gland (CG) were studied in male viscacha, a seasonally reproductive wild rodent. Two histologically well-defined zones, peripheral and central, were identified in the prostate, according to their relationship with the urethra. The epithelial cells were periodic acid-Schiff (PAS)-positive in the central zone and alcian blue negative in the two zones. The SV are a paired gland, tubular, of tortuous aspect and formed by radial layers. The bulbourethral glands were paired, formed by tubuloalveolar acini and surrounded by a thick layer of skeletal muscle. The CG was multilobulated. The large adenomers showed PAS-positive epithelium and were negative to alcian blue. Androgen receptors in the P, SV and coagulating gland showed variations in their distribution with immunohistochemistry heterogeneous pattern. Finally, the reproductive system accessory glands of male viscacha may be considered as a novel and interesting model for the study of seasonal reproduction in photoperiod-dependent animals.

Introduction

In most male mammals, the accessory glands of the reproductive system include the prostate (P), the seminal vesicles (SV) and the bulbourethral glands (BG). Some species such as rabbit, rat, hamster and monkey also exhibit a coagulant gland (CG), which is absent in humans.

The localization, shape, size, number and function of the secretion products of the accessory glands vary with the different species (Aumüller and Seitz, 1990; Frandson and Spurgeon, 1995). During ejaculation, spermatozoa leave the epididymis and go through the vas deferens, urethra and penis, where the secretions of P, SV, BG and CG play a main role in the chemical composition and volume of ejaculated semen.

Androgens are necessary for the prenatal and postnatal development of the male accessory sexual glands, with testosterone being the main androgen circulating in blood (Luke and Coffey, 1994; Thompson, 2001). Dihydrotestosterone (DHT), the active form of testosterone, is a potent androgenic metabolite produced in P and SV; the reduction of testosterone takes place by the action of a specific enzyme, 5 α-reductase. The action of androgens or DHT on the gland cells depends on the specific union to an androgen nuclear receptor (AR) and the subsequent formation of the DHT-AR complex. On the other hand, it has been demonstrated that the development, growth and secretory function of these glands are stimulated by serum testosterone (Wahlqvist et al., 1996).

Our experimental model is the viscacha (*Lagostomus maximus maximus*), a wild South American rodent of nocturnal habits. Its physiology and behaviour vary throughout the year depending on environmental signals such as photoperiod length, temperature, rain regime, food availability and social interactions (Llanos and Crespo, 1954; Redford and Eisenberg, 1992; Jackson et al., 1996). Studies performed in our laboratory have shown that this rodent is a seasonal reproductor, the environmental photoperiod being the main synchronizer of the annual reproductive cycle through the pineal gland and

its main hormone, melatonin (Dominguez et al., 1987; Fuentes et al., 1991, 2003; Pelzer et al., 1999). In its habitat, the adult male presents a three-period reproductive cycle. The period of highest reproductive activity takes place in summer and in the start autumn, followed by a short period of regression gonadal in winter. Subsequently, the reproductive system gradually recuperates during spring until it reaches again its maximum activity in summer (Muñoz et al., 1997, 1998b, 2001). A detailed descriptive study of viscacha testes (Muñoz, 1998a) and epididimys (Fuentes et al., 1991; Aguilera Merlo et al., 2005a; Aguilera-Merlo et al., 2009) has contributed with important information on the reproductive biology of this rodent. However, there are no reports on the morphophysiology of the viscacha accessory glands, which have been extensively described in other species such as rat (Jesik et al., 1982), hamster (Toma and Buzzell, 1988), dog (Niu et al., 2003), rabbit (Vásquez and del Sol, 2002), chinchilla (Adaro et al., 1999, 2001), anantolial souslik (Çakir and Karataş, 2004) and boar (Badia et al., 2006a,b).

The purpose of this work was to describe the anatomical, histological and AR characteristics of P, SV, BG and CG in male viscacha and to study the immunohistochemical distribution and localization of AR in these glands. It is expected that our results will permit to guide further histophysiological and biochemical studies of the reproductive cycle of this rodent.

Materials and Methods

Animals

Ten male adult viscachas (*Lagostomus maximus maximus*) weighing 5–8 kg were captured in summer, in their habitat near San Luis, Argentina (33°20′ south latitude 760 m altitude). The animals were anaesthetized intraperitoneally with 25 mg/kg of sodium thiopental (Sigma-Aldrich Co., St Louis, MO, USA) and sacrificed.

Anatomical and histological study

The male reproductive system accessory glands were removed and placed in glutaraldehyede 5% (Merck, KGaA, Darmstadt, Germany) and dissected in Petri dishes. For light microscopy evaluation, the samples were fixed in Bouin's fluid, dehydrated in an increasing ethanol series, and embedded in paraffin. Sections, 3–4 μm thick, were stained using the following histological and histochemical methods: haematoxylin–eosine (H&E) and van Gieson as a general stain, periodic acid-Schiff (PAS) specific for neutral glycoconjugates and alcian blue pH 2.5 (Biopack, Capital Federal, Buenos Aires, Argentina) specific for acid glycoconjugates, alcian blue pH 1.0 specific for sulphated acid mucosubstances. All stained sections were observed using a Nikon Eclipse E200 light microscope (Melville, NY, USA)

.

Immunohistochemistry

The tissue sections were first deparaffinized with xylene and hydrated through decreasing concentrations of ethanol. They were incubated for 20 min in a solution of 3% H_2O_2 in water to inhibit endogenous peroxidase activity. Next, they were rinsed with distilled water and phosphate-buffered saline (PBS, 0.01 M, pH 7.4). Non-specific binding sites for immunoglobulins were blocked by incubation for 20 min with normal goat serum diluted in PBS containing 1% bovine serum albumin, 0.09% sodium azide, 0.1% Tween-20. Sections were then incubated overnight in a humidified chamber at 4°C with the rabbit polyclonal antibody AR (N-20) (Santa Cruz Biotechnology, Inc., Santa Cruz, CA, USA). They were then rinsed with PBS for 10 min, and the immunohistochemical visualization was carried out using the Super Sensitive Ready-to-Use Immunostaining Kit (BioGenex, San Ramon, CA, USA) at 20°C. The Biotin-Streptavidin Amplified system (B-SA) was used as follows: sections were incubated for 30 min with diluted biotinylated anti-mouse IgG, and after being washed in PBS, they were incubated for 30 min with horseradish peroxidase-conjugated streptavidin, and finally washed in PBS. The reaction site was revealed by 100 μl 3,3′-diaminobenzidine tetrahydrochloride (DAB) chromogen solution in 2.5 ml PBS and 50 μl H_2O_2 substrate solution. The sections were dehydrated and mounted.

To confirm the specificity of the immunoreactive procedures, two controls of the primary antibody were made: (1) omission of primary antibody and (2) adsorption of primary antibody with homologous antigen. No positive structures or cells were found in these sections. Prostates of rats were used as positive controls.

Morphometric analysis

For light microscopy assessments, sections stained with H&E were examined. For each animal, from 3 blocks per gland, 25 transverse sections were analysed. Measurements were made with a micrometer ocular using an objective of ×10 and ×40 (total magnification: ×100 and ×400 respectively). The following measurements were performed in paraffin sections: luminal diameter, epithelium height, epithelial fold height and thickness of muscular layer.

The results were expressed as mean ± standard error of the mean (SEM) for all data sets. In prostate, the peripheral and central zones were evaluated using Student's *t*-test. A probability of <0.05 was assumed to be significant.

Results

Prostate gland

Anatomical description

The prostate was found to be a non-paired gland of ochre colour and soft consistency (Fig. 1a,b), located in caudal position with respect to the bladder, above the floor of the perineum, ventrally with respect to the rectum and dorsally with respect to the coxal bones. This gland was formed by two partially lateralized lobules, linked by an isthmus and without completely surrounding the urethra (Fig. 1b,c) and exhibited four well-defined regions: cranial, caudal, ventral and dorsal. The cranial region was related to the urinary bladder, the CG, the SV and the deferent ducts (Fig. 1b). The caudal region contacted the pelvic urethra. The ventral region was related to the bladder portion and beginning of the urethra (Fig. 1c). The dorsal region was located in a position anterior to the rectum.

Histological and histochemical description

Serial histological cuts performed on the whole prostate gland revealed two well-differentiated gland regions considering the distance between the gland adenomers and the urethra: a peripheral zone (Fig. 2a) and a central

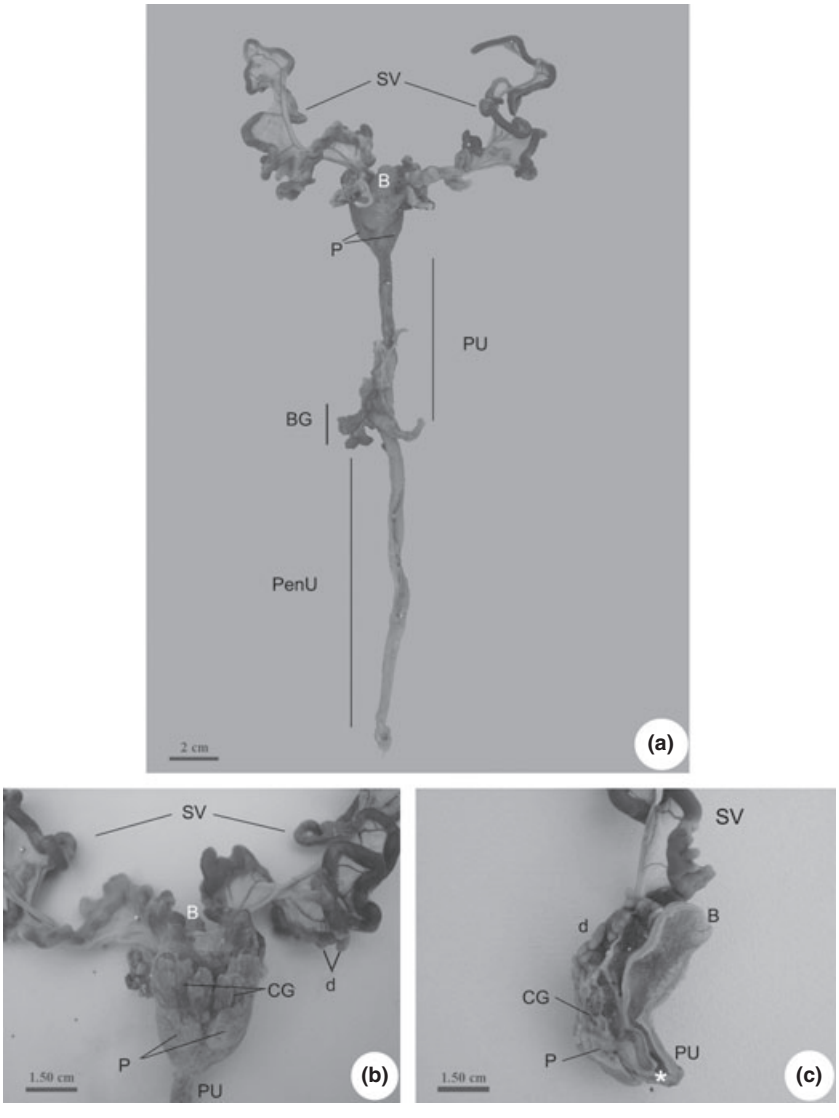

Fig. 1. Anatomy of the accessory reproductive glands of male viscacha (attached organs were removed). (a) Ventral view of the male urogenital system of viscacha. SV, seminal vesicle; B, bladder; P, prostate; PU, pelvic urethra; BG, bulbourethral gland; PenU, penile urethra. (b) Dorsal view of the seminal vesicle (SV), prostate (P), and coagulant gland (CG). Evaginations (d) in the initial portion of the seminal vesicle are observed. B, bladder; PU, pelvic urethra. (c) Cross-section through longitudinal prostate (P) and bladder (B). This image shows prostate (P), coagulant gland (CG) and seminal vesicle (SV) independently emptying into the urethral (asterisk). PU, pelvic urethra; BG, bulbourethral gland; PenU, penile urethra.

zone (Fig. 2e). Both zones possessed an organized parenchyma with abundant adenomers and fibromuscular stroma. A thin fibrous capsule surrounded the gland structure. The main morphological and histochemical differences between these zones were the following:

Peripheral zone (PZ): This region was the most distant from the urethra and was characterized by adenomers with large lumen and scarce folds. Surrounding the adenomers a thin layer of smooth muscle and collagen fibres was observed. Blood vessels and nerve ganglions were also observed (Fig. 2b). The epithelium was low cubic, with nuclei in central position, loosely structured chromatin and evident nucleolus (Fig. 2c). The PAS histochemical study revealed that the epithelial cells were negative for neutral glycoproteins. The secretion contained in the lumen of the adenomers was PAS positive (Fig. 2d). The alcian blue technique demonstrated that these cells do not possess acid or sulphated glycoproteins.

Central zone (CZ): This region was the closest to the urethral duct. It exhibited adenomers with reduced lumen, surrounded by fibromuscular tissue which was more developed than that of the PZ. The gland epithelium was cylindrical pseudostratified and formed abundant long folds that projected to the glandular lumen (Fig. 2e). The cylindrical epithelial cells with elongated nucleus were predominant, with lax chromatin and evident nucleolus (Fig. 2f). Histochemical analysis revealed scarce PAS-positive cells and the secretion con-

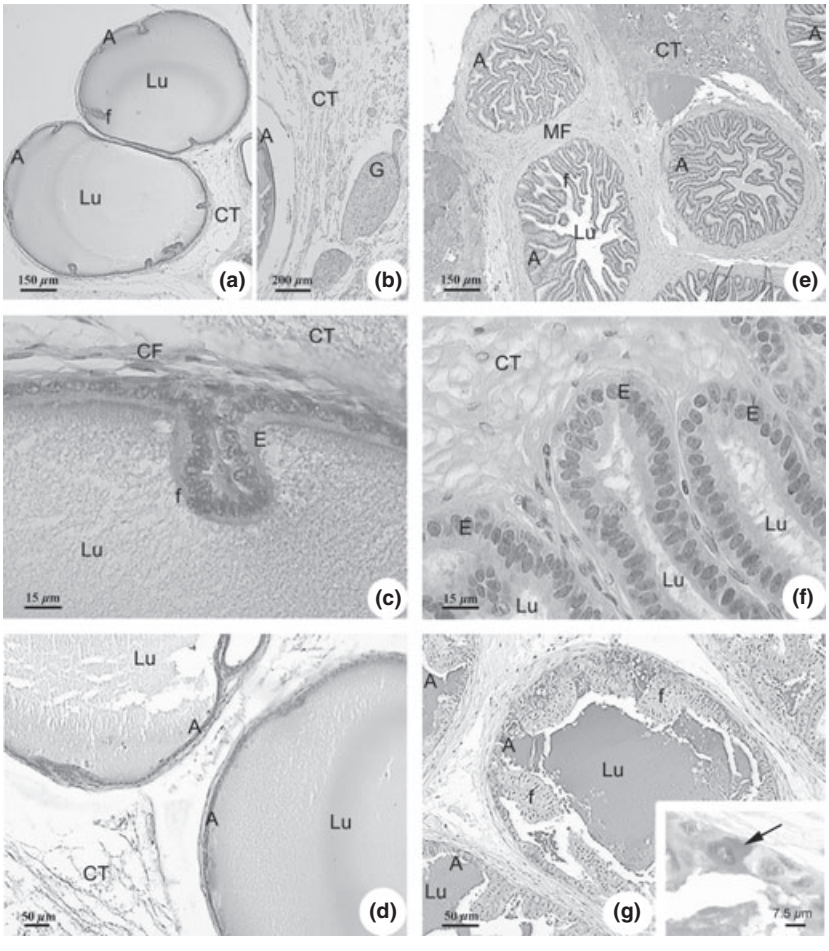

Fig. 2. Histological characteristic of peripheral zone (a–d) and central zone (e–g) of prostate. (a) Adenomers (A) of Peripheral zone show a large and regular lumen (Lu) with few epithelial folds (f). CT, connective tissue. H&E ×40. (b) Details of the connective tissue (CT) in contact with adenomers (A). G, nerve ganglions. H&E ×100. (c) Higher magnification of the cubic epithelium (E) observed in the peripheral zone. CF, collagen fibres; CT, connective tissue; Lu, lumen; f, fold. H&E ×400. (d) Adenomers (A) show PAS-positive reaction in the lumen secretion (Lu). CT, connective tissue. H-PAS ×250. (e). Adenomers (A) of central zone exhibit abundant folds (f) projected into the lumen (Lu). MF, muscle fibres; CT, connective tissue. H&E ×40. (f) Image of the pseudostratified cylindrical epithelium (E). Lu, lumen; CT, connective tissue. H&E ×400. (g) PAS-positive secretion of adenomers (A) of central zone. Lu, lumen; f, fold. H&E ×400. Inset: Epithelial cell (arrow) showing PAS-positive reaction. H-PAS ×1000.

tained in the lumen was intensely stained (Fig. 2g and inset). Alcian blue reaction was negative both in the epithelium and in the luminal content.

Morphometric analysis

Table 1 shows the morphometric analysis of the parameters corresponding to luminar diameter, height of epithelial cells, length of mucosa folds and thickness of the muscle layer, performed on both zones of the prostate gland. In the PZ, the morphometric evaluation showed large adenomers with short epithelium and few folds, and reduced muscle layer thickness, in relation to that observed in the CZ.

Table 1. Structural parameters of the different zones of viscacha prostate

Parameters	Central zone (μm)	Peripheral zone (μm)
Luminal diameter	435 ± 50.32	775 ± 43.43*
Epithelium height	13.6 ± 0.64	11.2 ± 0.44*
Epithelial fold height	165.68 ± 6.40	87.2 ± 3.44*
Thickness of muscular layer	87 ± 3.4	40 ± 2.8*

The values are expressed as mean ± SEM. The significant differences were determined by Student's *t*-test. *$P < 0.001$ perpheric zone versus central zone by Student's *t*-test.

Immunohistochemistry for androgen receptor

In the adenomers, the immunostaining observed in the gland parenchyma varied between the PZ (Fig. 3a) and the CZ (Fig. 3c). In the PZ adenomers, the nuclei of numerous epithelial cells were immunostained (Fig. 3b). On the other hand, in the CZ adenomers, few immunostained epithelial cells in the nuclei and cytoplasm were observed. In this zone, most of the cells exhibited intense heterogeneous immunostaining in the cytoplasm, while a lower proportion of cells were stained in the apical region (Fig. 3d). Smooth muscle fibres and fibroblasts in both glandular zones presented androgen receptor staining in the nuclei.

Seminal vesicles

Anatomical description

The viscacha SV were found to be a paired, of whitish colour, elongated and tortuous in shape (Fig. 1a). Both glands independently emptied into the urethral light. In the initial portion, the gland walls exhibited abundant evaginations in the form of blind pouches (Fig. 1b and c).

Histological and histochemical description

The SV were tubular glands formed by three radially arranged histological layers: mucosa, muscular and adventitia (Fig. 4a). The mucosa formed folds of variable

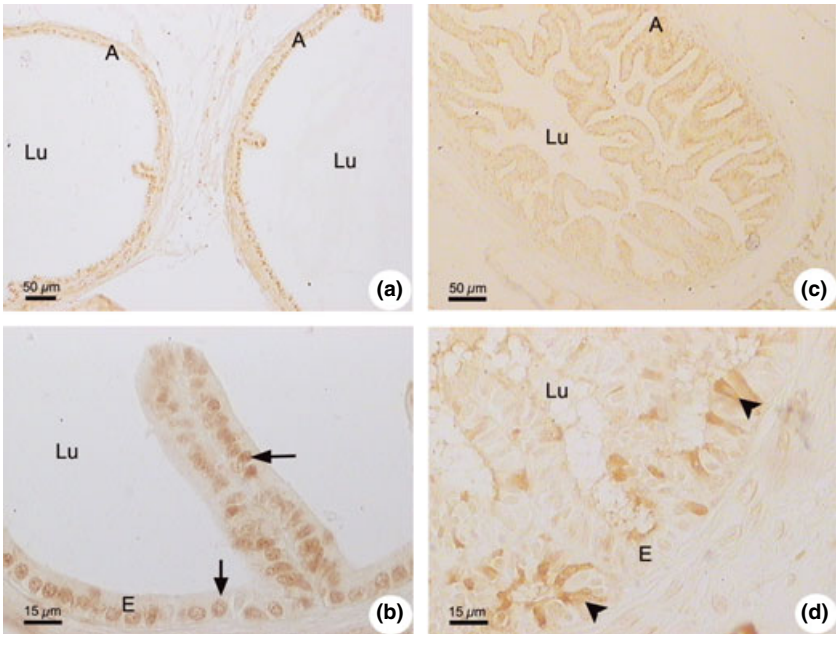

Fig. 3. Immunohistochemical localization of androgen receptor in prostate of viscacha. (a, b) Adenomers (A) of peripheral zone show numerous epithelial cells with immunostained nuclei (arrows). (b) Higher magnification of image (a). Magnification (a) ×100, (b) ×400. (c, d) Image of central zone. Few immunostained epithelial cells are observed in relation to a peripheral zone. The cytoplasmic pattern is heterogeneous (arrowheads). Magnification (c) ×100, (d) ×400.

length (ranging between 56 ± 12.2 μm and 96 ± 10 μm) that extended to the lumen. These folds branched out and anastomosed, forming secondary folds. The epithelium was cylindrical, pseudostratified and its height was approximately 6.6 ± 1.6 μm. It was formed by cylindrical cells with elongated nucleus, moderately condensed chromatin and evident nucleolus (Fig. 4b). In the epithelium base, there were basal cells of elongated shape with round or ovoid nucleus, similar to those described for the epididymis of this rodent (Aguilera-Merlo et al., 2009). The lumen was large and contained abundant secretion of homogeneous aspect. The muscular layer was approximately 59.2 ± 18.8 μm thick and was mainly formed by smooth muscle fibres and collagen fibres. Surrounding these structures, there was a thin adventitia of lax connective tissue (Fig. 4a). Both the epithelium and the secretion were negative for PAS and alcian blue.

Immunohistochemistry for androgen receptor

The glandular epithelium cells were AR positive, with a less intense staining than that observed in prostate. The ARs were localized in the nucleus of epithelial cells and smooth muscle cells. In the connective tissue, scarce fibroblastic-like stromal cells were found to express AR (Fig. 4c).

Bulbourethral glands

Anatomical description

These were paired tubuloalveolar glands, located dorsally with respect to the final portion of the pelvic urethra. They were small and spheroid, with thick consistency, and contained a sticky, whitish, viscous and abundant secretion product (Fig. 1a).

Histological and histochemical description

These glands were surrounded by a thick layer of skeletal muscle and dense connective tissue. Numerous trabecules originated from the capsule, dividing the gland into lobules, 462 ± 37.65 μm wide and 854 ± 64.64 μm thick (Fig. 5a). Each lobule was formed by acini and excretory ducts separated by scarce connective tissue. The acini were ovoid (69.72 ± 15 μm × 124 ± 30.28 μm) and composed of a simple cylindrical epithelium, except for the area close to the urethral orifice, where the epithelium was cylindrical pseudostratified. The epithelium height was 20.2 ± 0.32 μm. All the epithelial cells were characterized by a nucleus in basal position, flattened shape, lax chromatin and evident nucleolus (Fig. 5b). The glandular lumen was small, of irregular shape and contained an eosinophil secretion. The excretory ducts were of variable size (172.8 ± 26.32 μm × 334.4 ± 36.88 μm) and lined by an epithelium similar to that of the acini. This gland

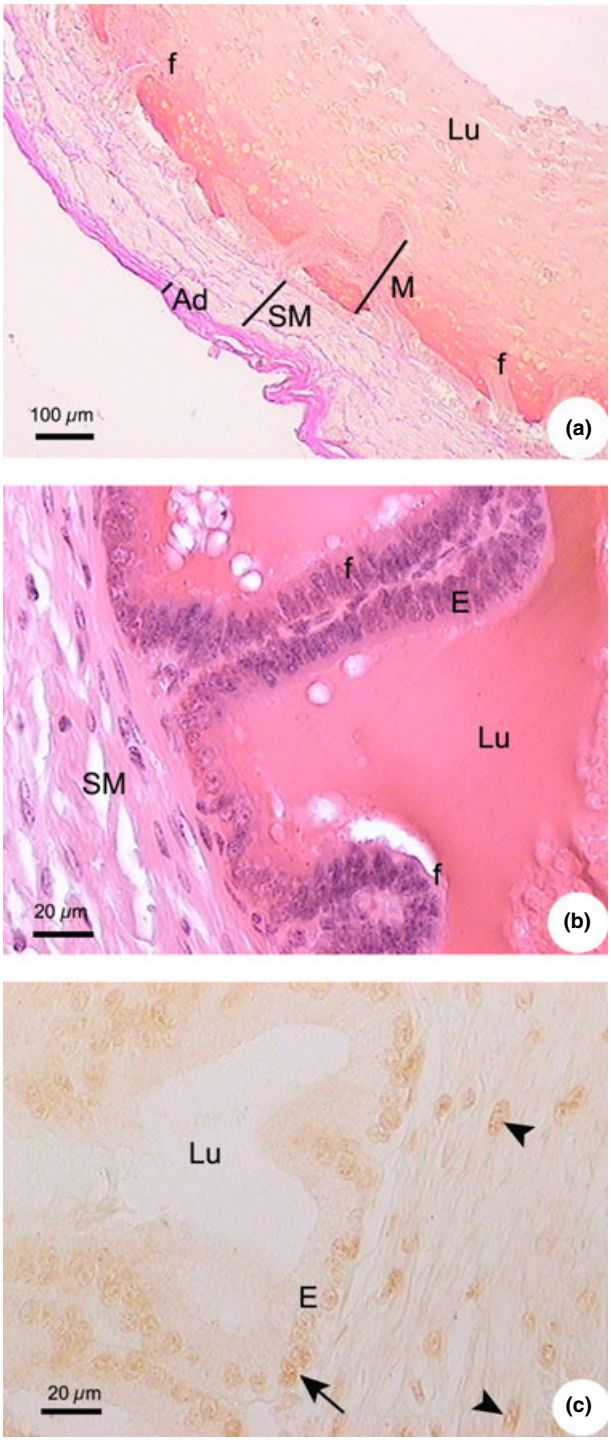

Fig. 4. Seminal vesicle of male viscacha. (a) Image shows the radial disposition of Santa Cruz Biotechnology the glandular histological layers. M, mucosa; SM, smooth muscle; Ad, adventitia; Lu, lumen; f, fold. van Gieson ×100. (b) Folds (f) of pseudostratified cylindrical epithelium (E). SM, smooth muscle; Lu, lumen. H&E ×400. (c) Immunohistochemistry for androgen receptors. The immunostaining is observed in the nucleus (arrow) of epithelial cells (E). Also, the smooth muscle cells (arrowhead) show immunoreaction ×100.

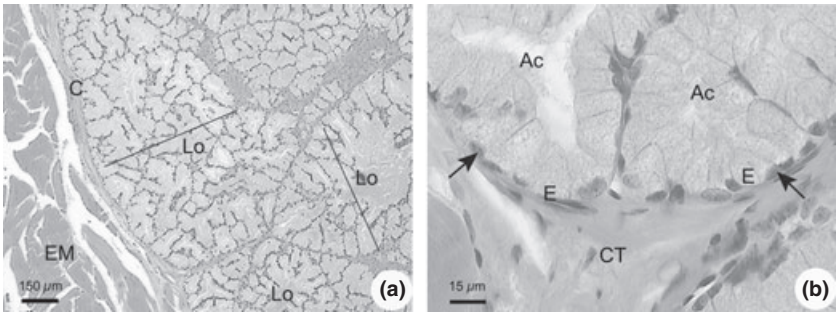

Fig. 5. Bulbourethral glands of male viscacha. (a) The glands are divided into lobules (Bar-Lo) and surrounded by a capsule (c) of connective tissue. EM: skeletal muscle. H&E ×100. (b) The glandular acini (Ac) are lined by single cylindrical epithelium (E). The nuclei (arrows) are localized in a basal position. CT, connective tissue. H&E ×400.

possessed scarce connective tissue surrounding the above described structures.

The histochemical study showed negative reaction to PAS and alcian blue.

Immunohistochemistry for androgen receptor

The immunohistochemistry of AR was negative in the epithelial cells of glandular acini. Only slight staining was observed in the fibroblasts nuclei (not shown).

Coagulant gland

Anatomical, histological and histochemical description

The CG was located on the upper part of the prostrate and it was found to have ducts that independently opened into the urethra (Fig. 1b).

In this gland, large adenomers (ranging between 1500 ± 158.4 μm and 2000 ± 186.7 μm) surrounded by a thin layer of smooth muscle were observed (Fig. 6a). The epithelium formed folds of variable length (approximately 134.25 ± 19.76 μm). The epithelial cells were low cubic and about 9 ± 1.4 μm high. The nuclei, located in the cell centre, were small and of condensed chromatin (Fig. 6b). The lumen contained abundant secretion of homogeneous aspect and was intensely PAS-positive. The reaction to alcian blue was negative.

Immunohistochemistry for androgen receptor

The ARs were expressed in the adenomers epithelium with cytoplasmic and nuclear staining (Fig. 6c.)

Discussion

Numerous descriptive studies of the male reproductive system accessory glands have been carried out in species such as rabbit (Holtz and Foote, 1978; Vásquez and del Sol, 2002), chinchilla (Adaro et al., 1999; Cepeda et al., 2006), cat (Reighard and Jennings, 1966), dog (Niu et al., 2003), rat (Jesik et al., 1982; Hayashi et al., 1991), hamster (Toma and Buzzell, 1988) and mongolian gerbil (Pinheiro et al., 2003).

The macroscopic morphology of the viscacha prostate is similar to that described for chinchilla (Cepeda et al., 2006), cat (Reighard and Jennings, 1966) and dog (Miller et al., 1965). It presents two lobules joined by an isthmus which do not completely surround the urethra. On the other hand, it is different from that of rodents such as rat, in which the gland is formed by two lateral lobules, dorsal and ventral (Jesik et al., 1982; Hayashi et al., 1991); or rabbit, in which the prostatic complex is formed by a proprostate, a prostate and paraprostate (Holtz and Foote, 1978).

The histological study of the viscacha prostate gland demonstrated the presence of two regions, CZ and PZ, with different histological and histochemical characteristics. In the PZ, there are tubulo-alveolar adenomers of wide and regular luminal diameter and lined by a prismatic epithelium, while in the CZ, the luminar diameter is smaller, the epithelium is higher and forms folds. Both regions were PAS-positive with variable intensities, which confirm the presence of neutral glycoproteins. These results differ from those reported by Vásquez and del Sol (2002) for rabbit and by Cepeda et al. (2006) for chinchilla, which, like viscacha, belongs to the Chinchillidae family. In these species, the histochemical reaction to PAS is negative for the prostate portion of the prostatic complex in rabbit and for the prostate central zone in chinchilla. On the other hand, the reaction to alcian blue was negative in both zones of the viscacha prostate, indicating the absence of acid and sulphated glycoproteins in the secretion. This result was similar to that described by Cepeda et al. (2006) for chinchilla, but differs from reports by Vásquez and del Sol (2002), who observed positive reaction to alcian blue in the prostatic portion of rabbit.

The variations observed within the gland zones of the viscacha prostate, both at the height of the epithelium and in the histochemical reactions, suggest heterogeneity in the secretory pattern of this gland or the existence of

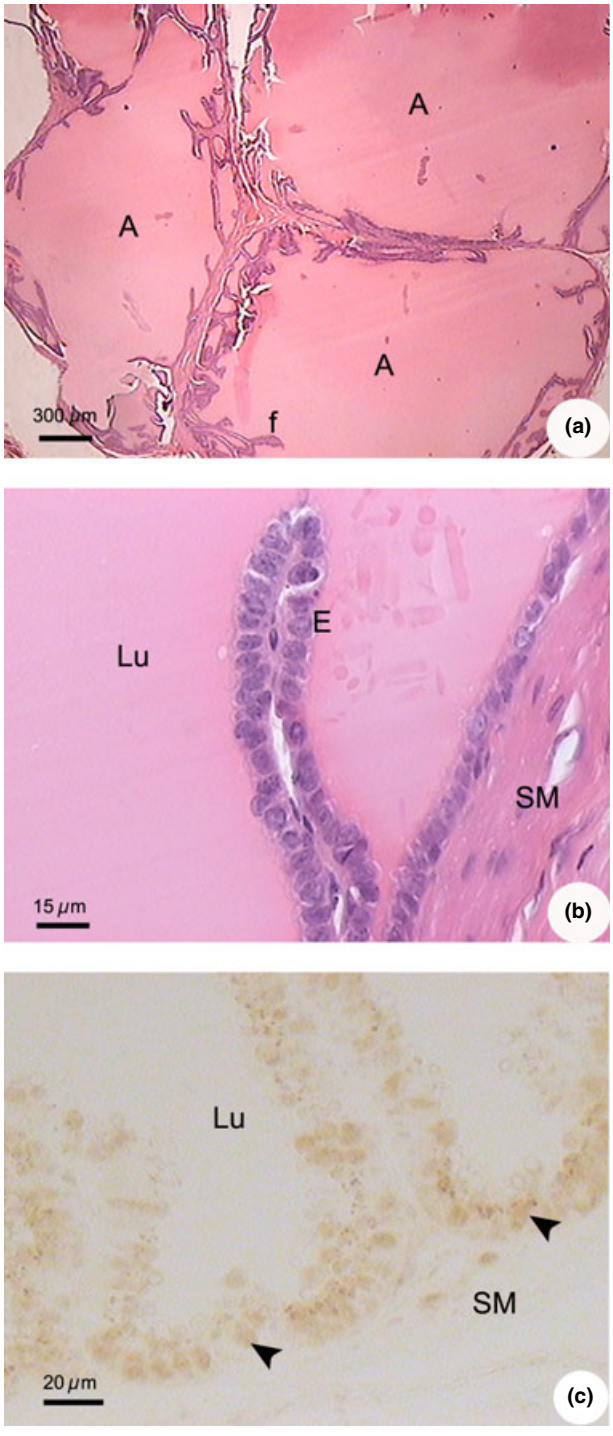

Fig. 6. Coagulant gland of male viscacha. (a) Micrograph shows adenomers (A) with short folds (f) projected into the lumen. H&E ×100. (b) Higher magnification of the cubic low epithelium (E) of the adenomers. Lu, lumen; SM, smooth muscle. H&E ×400. (c) Immunohistochemistry for androgen receptor. The immunostaining is observed in the nucleus and the cytoplasm of epithelium (arrowheads). Lu, lumen; SM, smooth muscle. H&E ×100.

different secretor cycle stages. This has also been reported by Cepeda et al. (1999) for chinchilla and Hayashi et al. (1991) for rat.

Immunohistochemical studies of AR in the prostate of viscacha demonstrate that the glands PZ and CZ exhibit different expression and immunostaining patterns. The PZ expresses abundant AR localized exclusively in the nucleus, while in the CZ, staining is less intense than in the PZ, and immunostaining is expressed in the cytoplasm of epithelial cells. These findings suggest that the cytoplasmic expression of AR in the CZ could indicate a lower stimulation of the hormone on this region (Hager et al., 2000). This would indicate the existence of a differential regulation depending on the gland zone, with the PZ being more dependent on the androgen levels than the CZ. Similar results have been reported for different lobules of the prostate in rat (Prins, 1989). In agreement with the studies performed by Takeda et al. (1990) in other species such as rat, mouse and humans, our results confirm a close relationship between the elevated number of receptors and the higher secretory activity of the gland cells. The cells that do not exhibit AR are probably in an inactive functional phase or represent the reserve population in the epithelium.

The SV in viscacha are formed by two elongated structures with evaginations only in the initial portion of each gland, similar to descriptions in chinchilla, although lower in number (Adaro et al., 2001). On the other hand, rabbit SV do not present evaginations (Holtz and Foote, 1978) and in boar, various lobules have been described (Badia et al., 2006a,b). Histochemical reaction to PAS and alcian blue are negative in the epithelial cells and the secretion, indicating absence of neutral and acid glycoproteins and sulphated mucopolysaccharides. These data are similar to those reported by Oróstegui et al. (2000) in chinchilla.

In our experimental model, AR immunostaining in the epithelium and the stroma of SV suggests an androgenic dependence of the glands. It is likely that there exists a paracrine control between the stroma and the mucosa of the glands (Prins et al., 1992; Welsh et al., 2010).

The presence and number of the BG vary in different mammal species. They are not present in dog (Krahmer et al., 1979), marsupials have three pairs (Barbour, 1981; Nogueira et al., 1984) and in rabbit, it is a non-paired gland (Vásquez and del Sol, 2001). In viscacha, the BG is paired and located on the dorsal surface of the caudal region, at the point where the pelvic urethra ends and the penis portion begins. The gland is surrounded by a thick layer of skeletal muscle fibres. Its localization in relation to the skeletal muscle might suggest that muscular contraction facilitates the expulsion of secretion, as has been

described for chinchilla (Cepeda et al., 1999) and boar (Badia et al., 2006a,b).

The BG were not immunostained for AR in the epithelium of the acini, but they did show a slight staining in the nuclei of the connective tissue cells. On the other hand, AR expression in the CG was observed in the epithelium of adenomers, with intense cytoplasmic staining.

The immunohistochemical study of AR in viscacha demonstrates that unlike other rodents, the distribution and localization of these receptors vary in the cells of the different accessory glands. These findings suggest that the accessory glands of the male viscacha reproductive system probably respond in a way different from the levels of circulating androgen.

In conclusion, this work constitutes the first anatomical, histological and immunohistochemical study of the accessory glands of the male viscacha reproductive system. It is expected that our results will contribute to guide further studies on the reproductive systems of this rodent. On the other hand, the accessory glands of viscacha may be considered as a novel and interest model for the study of seasonal reproduction in photoperiod-dependent animals.

Acknowledgements

We thank Mrs A. Bernardi and Mr J. Arroyuelo for their technical participation. This work was supported by Proyect 22Q/603, CyT. U.N.S.L.

References

Adaro, L., C. Oróstegui, R. Olivares, and S. Villanueva, 1999: Morphometric variations in male reproductor system in Chinchilla in captivity through a year (*Chinchilla laniger* Grey). Av. Prod. Anim. **24**, 91–95.

Adaro, L., J. Mendoza, R. Cepeda, and P. Oróstegui, 2001: Anatomo-radiographic study of the seminal vesicles of chinchilla (*Chinchilla laniger*) in captivity. Rev. Chil. Anat. **19**, 297–300.

Aguilera Merlo, C., E. Muñoz, S. Dominguez, L. Scardapane, and R. Piezzi, 2005a: Epididymis of viscacha (*Lagostomus maximus maximus*). Morphological changes during the annual reproductive cycle. Anat. Rec. **282**, 83–92.

Aguilera-Merlo, C., T. Fogal, T. Sator, S. Dominguez, M. Sosa, L. Scardapane, and R. Piezzi, 2009: Ultrastructural and biochemical seasonal changes in epididymal corpus and cauda of Viscacha (*Lagostomus maximus maximus*). J. Morphol. **270**, 805–814.

Aumüller, G., and J. Seitz, 1990: Protein secretion and secretory process in male accessory sex glands. Int. Rev. Cytol. **121**, 127–231.

Badia, E., M. Briz, E. Pinart, N. Garcia-Gil, J. Bassols, A. Pruneda, E. Bussalleu, M. Yeste, I. Casas, and S. Bonet, 2006a: Structural and ultrastuctural feature of boar bulbourethral glands. Tissue Cell **38**, 7–18.

Badia, E., M. Briz, E. Pinart, N. Garcia-Gil, J. Bassols, A. Pruneda, E. Bussalleu, M. Yeste, I. Casas, and S. Bonet, 2006b: Structural and ultrastuctural feature of boar seminal vesicles. Tissue Cell **38**, 79–91.

Barbour, R. A., 1981: Histology and histochemistry of the accessory reproductive glands in the male hairy-nosed wombat (*Lasiorhinus latifrons*). Histochemistry **72**, 133–148.

Çakir, M., and A. Karataş, 2004: Histo-anatomical studies on the accessory reproductive glands of the Anantolian Souslik (*Spermophilus xanthoprymmus*) (Mammalia: Sciuridae). Anat. Histol. Embryol. **33**, 146–150.

Cepeda, R., L. Adaro, P. Peñailillo, and C. Orostegui, 1999: Seasonal morphological variations of bulbourethral glands of chinchilla (*Chinchilla laniger,* Grey) in captivity. Rev. Chil. Anat. **17**, 59–66.

Cepeda, R., L. Adaro, and G. Peñailillo, 2006: Morphometric variations of *Chinchilla laniger* prostate and plasmatic testosterone concentration during its annual reproductive cycle. Int. J. Morphol. **24**, 89–97.

Dominguez, S., R. Piezzi, L. Scardapane, and J. Guzmán, 1987: A light and electron microscopic study of the pineal gland of the viscacha (*Lagostomus maximus maximus*). J. Pineal Res. **4**, 211–219.

Frandson, R., and T. Spurgeon, 1995: Anatomía y Fisiología de los Animales Domésticos, 5th edn. Mexico: Interamericana, Mcgraw-Hill.

Fuentes, L., N. Caravaca, L. Pelzer, L. Scardapane, R. Piezzi, and R. Guzmán, 1991: Seasonal variations in the testis and epididymis of viscacha (L.m.m.). Biol. Reprod. **45**, 493–497.

Fuentes, L., M. Møller, E. Muñoz, C. Calderón, and L. Pelzer, 2003: Seasonal variations in the expression of the mRNA encoding β1 – Adrenoceptor and AA-NAT enzyme, and in the AA-NAT activity in the pineal gland of viscacha (*Lagostomus maximus maximus*). Correlation with serum melatonin. Biol. Rhythm. Res. **34**, 193–206.

Hager, G., C. Lim, C. Elbi, and C. Baumann, 2000: Trafficking of nuclear receptors in living cells. J. Steroid Biochem. **74**, 249–254.

Hayashi, N., Y. Sugimura, J. Kawamura, A. Donjacour, and G. Cunha, 1991: Morphological and functional heterogeneity in the rat prostatic gland. Biol. Reprod. **45**, 308–321.

Holtz, W., and R. Foote, 1978: The anatomy of the reproductive system in male dutch rabbits (*Oryctolagus cuniculus*) with special emphasis on the accessory sex glands. J. Morphol. **158**, 1–20.

Jackson, J., L. Branch, and D. Villarreal, 1996: Lagostomus maximus. Mammalian Species **543**, 1–6.

Jesik, C., J. Holland, and C. Lee, 1982: An anatomic and histologic study of the rat prostate. Prostate **3**, 81–97.

Krahmer, R., L. Schröder, G. Michel, and G. Gutte, 1979: Anatomía de los Animales Domésticos, 2nd edn. Acribia: Zaragoza.

Llanos, A., and J. Crespo, 1954: Ecología de la vizcacha (*Lagostomus maximus maximus*) en el nordeste de la provincia de Entre Ríos. Revista de Investigaciones Agrícolas. Extra Nueva Serie nº **10**, 5–95.

Luke, M., and D. Coffey, 1994: The male sex accessory tissue. Structure, androgen, action, and physiology. In: The Physiology of Reproduction (E. Knobil and J. Neil, eds). New York: Raven Press. 1, pp. 1435–1487.

Miller, M., G. Christensen, and H. Evans, 1965: Anatomy of the Dog. Philadelphia: W. B. Saunders Company.

Muñoz, E., 1998a: Estudio estacional del compartimiento tubular e intersticial del testículo de vizcacha (Lagostomus maximus maximus). Papel de la melatonina en la ciclicidad reproductiva y su relación con el fotoperíodo. Tesis Doctoral. Biblioteca Central de la Universidad Nacional de San Luis, San Luis, Argentina.

Muñoz, E., T. Fogal, S. Dominguez, L. Scardapane, J. Guzmán, and R. Piezzi, 1997: Seasonal changes of the Leydig cells of viscacha (*Lagostomus maximus maximus*). A light and electron microscopy study. Tissue Cell **29**, 119–128.

Muñoz, E., T. Fogal, S. Dominguez, L. Scardapane, J. Guzmán, and R. Piezzi, 1998b: Stages of the cycle of the seminiferous epithelium of the viscacha (*Lagostomus maximus maximus*). Anat. Rec. **252**, 8–16.

Muñoz, E., T. Fogal, S. Dominguez, L. Scardapane, and J. Guzmán, 2001: Ultrastructural and morphometric study of the Sertoli cell of the viscacha (*Lagostomus maximus maximus*) during the annual reproductive cycle. Anat. Rec. **262**, 176–185.

Niu, Y. J., T. X. Ma, J. Zhang, Y. Xu, R. F. Han, and G. Sun, 2003: Androgen and prostatic stroma. Asian J. Androl. **5**, 19–26.

Nogueira, J., P. Campos, and M. Ribeiro, 1984: Histology, glycogen and mucosubstances histochemistry of the bulbourethral glands of the *Philader opossum* (Linnaeus, 1758). Anat. Anz. **156**, 321–328.

Oróstegui, P., G. Parraguez, A. Adaro, G. Peñailillo, and R. Cepeda, 2000: Histological and morphometric changes of the seminal vesicles of *Chinchilla laniger* (grey) in captivity induce by seasonal variations. Rev. Chil. Anat. **18**, 89–96.

Pelzer, L., C. Calderón, and J. Guzman, 1999: Changes in weigth and hydroxyindole-O-methyltransferase activity of pineal gland of the plains viscacha (*Lagostomus maximus maximus*). Mastozool. Neotrop. **6**, 31–38.

Pinheiro, P., C. Almeida, T. Segatelli, M. Martinez, C. Padovani, and F. Martinez, 2003: Structure of the pelvic and penile urethra – relatonship with the ducts of the sex accessory glands of the Mongolian gerbil (*Meriones unguiculatus*). J. Anat. **202**, 431–444.

Prins, G., 1989: Differencial regulation of androgen receptors in the separate rat prostate lobes: androgen independent expression in the lateral lobe. J. Steroid Biochem. **33**, 319–326.

Prins, G., M. Cecim, L. Birch, T. Wagner, and A. Bartke, 1992: Growth response and androgen receptor expression in seminal vesicles from aging tansgenic mice expressing human or bovine growth hormone genes. Endocrinology **131**, 2016–2023.

Redford, K., and J. Eisenberg, 1992. Mammals of the Neotropics: The Southern Cone, Vol 2. Chicago: The University of Chicago Press, pp. 430.

Reighard, J., and H. Jennings, 1966: Anatomy of the Cat. Holt, Rinehart and Winston. New York, Chicago-San Francisco, Toronto-London: Third and enlarged ed.

Takeda, H., G. Chodak, S. Mutchnic, T. Nakamoto, and C. Chang, 1990: Immunohistochemical localization of androgen receptor with mono- and polyclonal antibodies to receptor androgen. J. Endocrinol. **126**, 17–25.

Thompson, A., 2001: Role of androgen and fibroblast growth factors in prostatic development. Reproduction **121**, 187–195.

Toma, J., and G. Buzzell, 1988: Fine estructure of the ventral and dorsal lobes of the prostate in the young adult syrian hamster, *Mesocricetus auratus*. Am. J. Anat. **2**, 132–140.

Vásquez, B., and M. del Sol, 2001: Morphologic study of bulbourethral gland of the rabbit (*Oryctolagus cuniculus*). Rev. Chil. Anat. **19**, 221–228.

Vásquez, B., and M. del Sol, 2002: Prostatic complex in the rabbit (*Oryctolagus cuniculus*). Rev. Chil. Anat. **20**, 175–180.

Wahlqvist, R., E. Dahl, and K. Tveter, 1996: Effects of castration upon the morphology of the accessory sex organs of the male rat – a scanning electron microscopy study. Scanning Microsc. **10**, 1155–1162.

Welsh, M., L. Moffat, L. Jack, A. McNeilly, D. Brownstein, P. Saunders, R. Sharpe, and L. Smith, 2010: Deletion of androgen receptor in the smoth muscle of the seminal vesicles impairs secretory function and alters its responsiveness to exogenous testosterone and estradiol. Endocrinology **151**, 3374–3385.